Electronic supplementary information for:

Synthesis, characterization and ab initio investigation of a panchromatic ullazine–porphyrin photosensitizer for Dye-Sensitized Solar Cells.

Simon Mathew[a,b]*, *Negar Ashari Astani*[c], *Basile F.E. Curchod*[c,d], *Jared H. Delcamp*[a,e], Magdalena Marszalek[a,g], *Julien Frey*[a,f], *Ursula Rothlisberger*[c], *Mohammad Khaja Nazeeruddin*[a], *Michael Grätzel*[a]

[a] Laboratory of Photonics and Interfaces (LPI), École Polytechnique Fédérale de Lausanne (EPFL), CH-1015, Lausanne, Switzerland.

[b] Current Address: van 't Hoff Institute for Molecular Sciences, University of Amsterdam, Science Park 904, 1098 XH Amsterdam, The Netherlands.

[c] Laboratory of Computational Chemistry and Biochemistry (LCBC), École Polytechnique Fédérale de Lausanne (EPFL), CH-1015 Lausanne, Switzerland

[d] Current Address: Department of Chemistry, Stanford University, Stanford, CA 94305–4401, USA.

[e] Current Address: Department of Chemistry, University of Mississippi, University, MS 38677, USA.

[f] Current Address: Novaled GmbH, Tatzberg 49, 01307 Dresden, Germany.

[g] Current Address: Department of Physics and Astronomy, Faculty of Sciences, Vrije Universiteit Amsterdam, De Boelelaan 1081, 1081 HV, Amsterdam, The Netherlands.

Contents:

1. General information

All commercially available reagents were used as received. All reactions were carried out under a nitrogen atmosphere unless otherwise noted. Thin-Layer Chromatography (TLC) was performed with Merck KGaA pre-coated TLC silica gel 60 F_{254} aluminium sheets, visualizing with UV (254 nm) light where required. Flash column chromatography was performed using Merck Silica gel 60 (0.015–0.040 μm). NMR spectra were recorded on a Bruker Avance-400 (400 MHz), Bruker Avance III-400 (400 MHz) or Bruker DPX-400 (400 MHz) spectrometer and are reported in ppm using a solvent as an internal standard ($CDCl_3$ at 7.26 ppm). Peaks are reported as s = singlet, d = doublet, t = triplet, q = quartet, p = pentet/quintet, m = multiplet, br s = broad singlet; coupling constant (Hz); integration. UV-vis spectra were measured with a Hewlett-Packard 8453 UV–vis spectrophotometer. Emission spectra were recorded with a Fluorolog Horiba Jobin Yvon Model FL-1065. Cyclic voltammetry (CV) was measured with an Autolab Eco Chemie Voltmeter.

2. Synthetic details

Alkynyl Ullazine **2**:

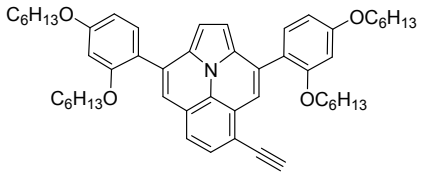

To a flame dried flask was added freshly prepared dibromomethyl-triphenylphosphonium bromide[1] (1.04 g, 2.02 mmol, 2.02 eq.) and THF (10 mL). In one portion, potassium *tert*-butoxide (213 mg, 1.90 mmol, 1.9 eq.) was added and the mixture stirred at ambient temperature for 3 minutes upon which the yellow solution turned yellow-brown. A solution of **1**[2] (770 mg, 1 mmol, 1.0 eq.) in THF (1.67 mL) was added to the reaction mixture via cannula, and the resulting mixture was stirred at room temperature for 10 minutes. The reaction was cooled to -78°C and potassium *tert*-butoxide (561 mg, 5.01 mmol, 5.0 eq.) was added in one portion following gradual warming to ambient temperature. After 1.5 hours, the reaction mixture was diluted with DCM and rinsed with water, dried ($MgSO_4$) and evaporated. The crude product was filtered through a pad of silica, eluting with DCM/hexane (1:1) and the solvent removed to afford the desired product (546 mg, 71%) as a yellow oil. ^{1}H NMR (400

MHz, $CDCl_3$) δ 7.72 (s, 1H), 7.60 (d, *J* = 8.0 Hz, 1H), 7.52 (d, *J* = 8.4 Hz, 1H), 7.48 (d, *J* = 8.4 Hz, 1H), 7.36 (d, *J* = 8.0 Hz, 1H), 7.29 (s, 1H), 6.92–6.86 (m, 2H), 6.67–6.58 (m, 4H), 4.05 (t, *J* = 6.8 Hz, 2H), 4.04 (t, *J* = 6.8 Hz, 2H), 3.97 (t, *J* = 6.3 Hz, 2H), 3.96 (t, *J* = 6.3 Hz, 2H), 3.43 (s, 1H),1.90–1.78 (m, 4H), 1.67–1.56 (m, 4H), 1.56–1.46 (m, 4H), 1.43–1.33 (m, 8H), 1.31–1.22 (m, 4H) 1.21–1.12 (m, 8H), 0.94 (t, *J* = 6.9 Hz, 6H), 0.76 (t, *J* = 6.9 Hz, 3H), 0.74 (t, *J* = 6.9 Hz, 3H). ^{13}C NMR (100 MHz, $CDCl_3$) δ 160.45, 160.43, 157.9, 157.8, 131.7, 131.5, 131.4, 131.0, 130.6, 127.9, 127.64, 127.56, 127.5, 126.4, 120.3, 120.1, 119.9, 117.7, 109.3, 107.04, 106.95, 105.10, 105.07, 100.62, 100.58, 83.0, 81.0, 68.64, 68.55, 68.2, 31.6, 31.42, 31.35, 29.7, 29.3, 29.0, 25.8, 25.71, 25.68, 22.6, 22.5, 22.4, 14.0, 13.9. HRMS (ESI-ToF-MS) m/z calculated for $C_{52}H_{66}NO_4$ $[M^+H]^+$: 768.4992, found 768.4990.

Dye **SM63**:

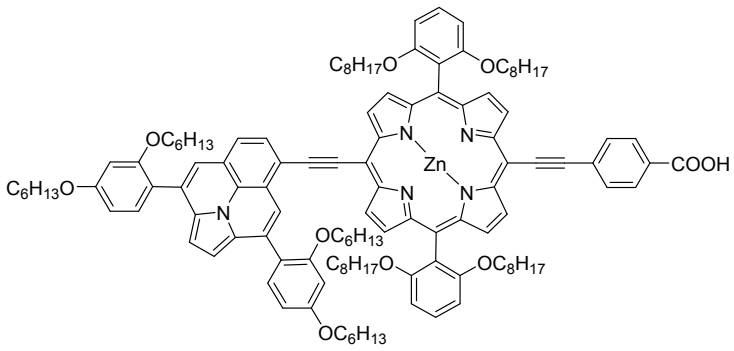

2 (45 mg, 0.0586 mmol), **3**[3] (0.1172 mmol, 140 mg, 2 eq.), $Pd(PPh_3)_4$ (5.0 mg, 0.004 mmol, 7mol%) and CuI (2.0 mg, 0.105 mmol, 18 mol%) were combined in a flask. After evacuation and filling with N_2, THF (15 mL) and Et_3N (1.5 mL) were introduced and the reaction mixture heated at reflux until no more **2** could be detected by TLC (silica, THF/hexane, 1:9). The solvents were evaporated and the residue purified by column chromatography (silica, THF/hexane, 1:9), isolating the monosubstituted product as the first brown fraction (confirmed by APPI-FTMS, m/z calculated for $C_{116}H_{146}BrN_5O_8Zn$ $[M]^+$: 1879.96463, found 1879.96096). The solvents were evaporated and combined with $Pd(PPh_3)_4$ (5.0 mg, 0.004 mmol, 7mol%), CuI (2.0 mg, 0.105 mmol, 18mol%) and 4-ethynylbenzoic acid (25.7 mg, 0.176 mmol, 3 eq.). the flask was evacuated and filled with nitrogen before THF (15 mL) and Et_3N (1.5 mL) were introduced and the reaction mixture heated at reflux for 3 hours. The solvents were evaporated

and the remaining solids purified by column chromatography (silica, DCM/MeOH, 19:1) to afford the pure product (30 mg, 26%) as a brown solid. ^{1}H NMR (400 MHz, $CDCl_3$) δ 9.71 (d, *J* = 4.4 Hz, 2H), 9.55 (d, *J* = 4.4 Hz, 2H), 8.80 (d, *J* = 4.4 Hz, 2H), 8.75 (d, *J* = 4.4 Hz, 2H), 8.41 (s, 1H), 8.27 (d, *J* = 7.2 Hz, 2H), 8.08 (d, *J* = 8.0 Hz, 1H), 8.01 (d, *J* = 7.2 Hz, 2H), 7.69 (d, *J* = 8.0 Hz, 1H), 7.68 (t, *J* = 8.4 Hz, 2H), 7.54 (d, *J* = 8.0 Hz, 2H), 7.37 (s, 1H), 7.01 (t, *J* = 8.4 Hz, 4H), 6.94 (d, *J* = 4.0 Hz, 1H), 6.91 (d, *J* = 4.0 Hz, 1H), 6.67–6.60 (m, 4H), 4.06 (t, *J* = 6.4 Hz, 4H), 3.98 (dd, *J* = 8.4, 6.8 Hz, 4H), 3.90–3.81 (m, 8H), 1.92–1.80 (m, 4H), 1.69–1.60 (m, 4H), 1.59–1.49 (m, 8H), 1.45–1.36 (m, 8H), 1.34–1.17 (m, 16H), 1.13–1.03 (m, 4H), 0.99–0.77 (m, 26H), 0.74–0.65 (m, 6H), 0.58–0.50 (m, 8H), 0.53 (t, *J* = 7.0 Hz, 12H), 0.47–0.37 (m, 8H). ^{13}C NMR (100 MHz, $CDCl_3$) δ 160.4, 160.3, 160.0, 158.0, 157.8, 151.7, 151.3, 150.43, 150.38, 132.2, 131.61, 131.58, 131.4, 131.2, 131.1, 131.0, 130.5, 130.2, 130.04, 130.00, 129.9, 129.5, 127.7, 127.6, 127.5, 127.1, 125.7, 121.5, 120.6, 120.5, 120.3, 120.1, 118.2, 114.9, 112.41, 112.37, 107.1, 106.8, 105.13, 105.07, 101.4, 100.6, 98.8, 98.1, 95.5, 94.5, 68.8, 68.6, 68.5, 68.14, 68.07, 31.9, 31.7, 31.6, 31.4, 31.2, 29.6, 29.4, 29.3, 29.0, 28.9, 28.7, 25.9, 25.8, 25.7, 25.5, 25.3, 22.7, 22.6, 22.5, 22.3, 22.1, 14.1, 14.0, 13.9, 13.8, 13.6. APPI-FTMS m/z calculated for $C_{125}H_{151}N_5O_{10}Zn$ $[M]^+$: 1946.07524, found 1946.07903.

3. Computational details:

Full geometry optimization of compounds SM63 and LD14 in their singlet ground state were performed with DFT using the M06[4] functional with the effective core potential and basis set LANL2DZ[5] for zinc, and a 6-31G*[6] basis set for the remaining atoms together with ultrafine grid, and tight geometrical convergence criteria implemented in Gaussian 09 package.[7] The polarizable continuum model (PCM) using the integral equation formalism variant (IEFPCM)[8] is employed for treating solvation effects. Being an aprotic solvent, the relative permittivity of 7.43 is applied for tetrahydrofuran (THF), which is the solvent used in this work. Bulky electronically passive alkoxy chains were replaced by methoxy groups. All the geometry optimizations were followed by frequency calculations for ensuring that the molecular configurations reached to a minimum of the ground state (and the first excited state for stoke shift calculation) potential energy surfaces. The choice of the M06 exchange-correlation functional for porphyrin-based dyes is justified in our earlier publication.[9] For each compound, LR-TDDFT/M06/IEF-PCM (THF) calculations were performed for the first 30 excited states, using the same basis set and xc-functional. M06 is capable of describing transitions with a

small amount of charge transfer (CT) character, which is the case in porphyrin-based dyes. Vertical ionization energy (IE) was computed at (U)DFT/M06 level of theory. Graphical representation of the molecules and their orbitals were obtained with the software VMD v.1.9.0.[10] The changes in electronic density between the ground state and the first electronic excited state were monitored by a density difference plot (Figure 6), which highlights the donor to acceptor CT character of the lowest energy transition. The geometries of different rotamers of SM63 with respect to the phenyl ring on the donor were optimized and the energy difference between them (0.05 eV) was below the error of the theoretical methods used. Geometries of both dyes were optimized in their ground and first excited state. The stoke shift was then calculated by subtracting the energies of the first absorption and emission transitions of the ground state and the first excited state optimized structures, respectively. LR-TDDFT was used for optimizing the structure in its first excited state. Two extra excited states (3 in total) were included in TD expansion for the geometry optimization in the first excited state. Interestingly, the slightly bent structure of SM63 was ~ 3 kcal/mol lower in energy than that of the planar structure. Carrying a bulky donor, SM63 gains stability via van der Waals interactions between ullazine and the alkoxyphenyl group at porphyrin *meso*-position. Unlike most of the porphyrin-based dyes that gain stability from its well-conjugated planar structure, SM63 sacrifices part of the electronic conjugation for sake of van der Waals interactions. To assess this hypothesis we tried BLYP[11] functional, which is known not to reflect weak dispersion interactions.[12,13] Indeed BLYP functional estimated the planar structure to be more stable by ~4 kcal/mol. This however, was reversed once Grimme-D2[14] empirical dispersion correction form of BLYP was used. Including the dispersion correction, the bent structure was estimated ~7 kcal/mol more stable than the planar one. In addition we tested several other geometries looking for possible global minimum. Among them the reported bent structure had the deepest minimum.

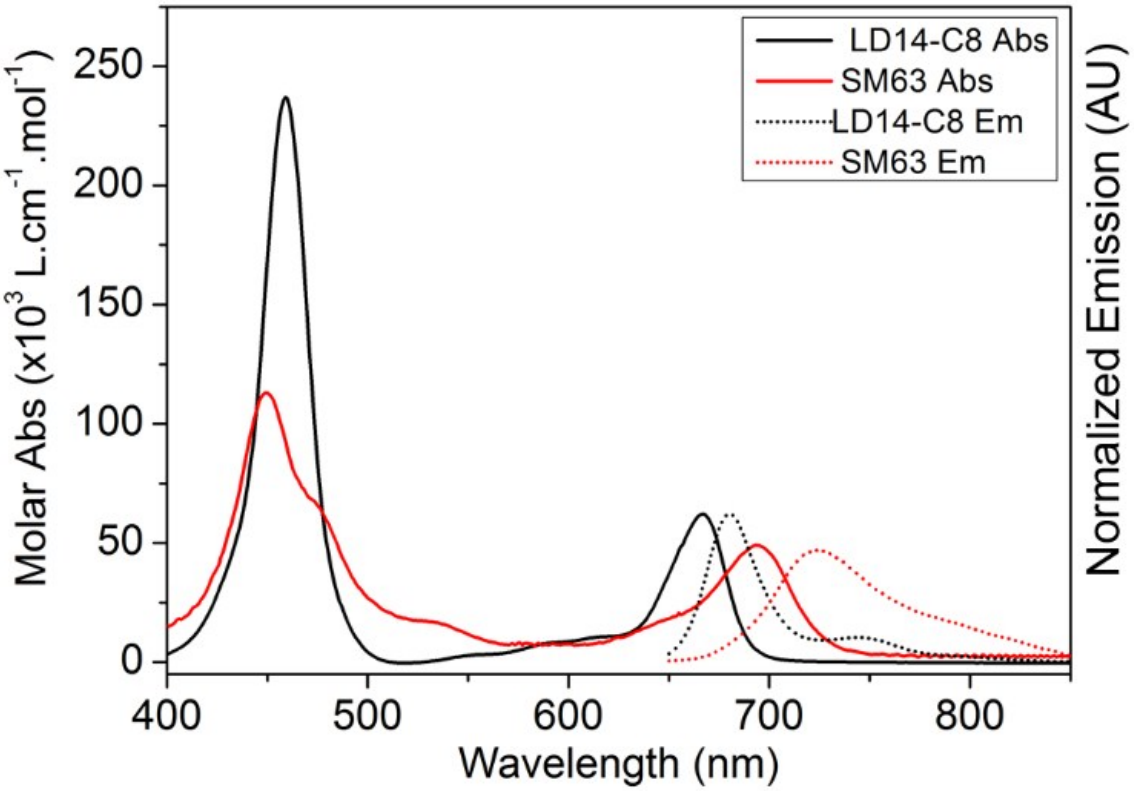

4. Steady state absorbance and fluorescence spectra of LD14-C8 and SM63

Figure S1. Steady-state absorbance (solid lines) and fluorescence spectra (dotted lines) of LD14-C8 (black) and SM63 (red) in THF with λ_{ex} = 475 nm (SM63) or 660 nm (LD14-C8).

5. Photovoltaic data for the optimization of DSCs employing SM63

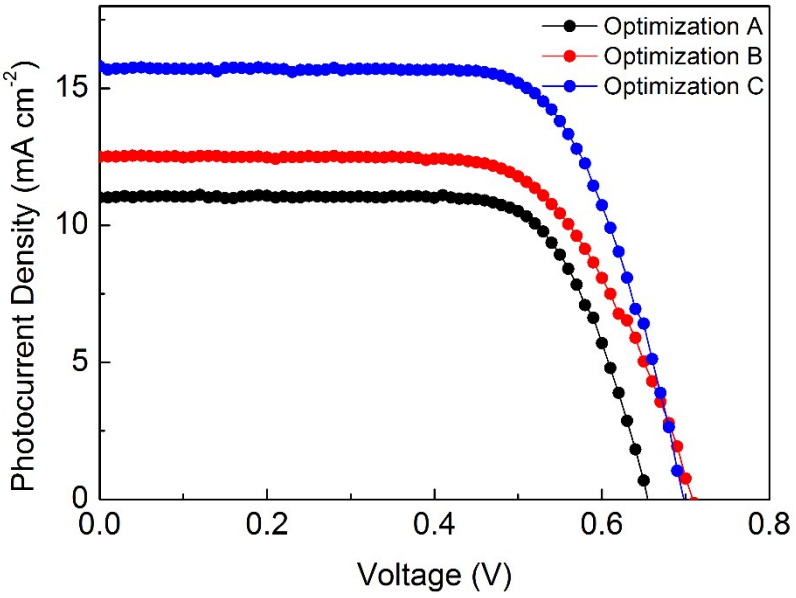

Figure S2. J–V curve of DSCs employing SM63: A) Black - Dipping Time 30 min; (THF/EtOH, 1:4); 0.2 mM CDCA. B) Red - Dipping Time 60 min; (THF/EtOH, 1:4); 2 mM CDCA. C) Blue - Dipping Time 60 min; (Toluene/EtOH, 1:1); 2 mM CDCA.

Table S1. Summary of conditions and photovoltaic parameters for data for the optimization of DSCs employing SM63.

Optimization Step	Solvent (ratio)	Dip Time (min)	CDCA (mM)	J_{SC} (mA cm^{-2})	V_{OC} (V)	FF	PCE (%)
Dipping time	THF/EtOH (1:4)	30	0.2	10.9	0.66	0.73	5.25
		60	0.2	10.4	0.66	0.53	3.65
		90	0.2	8.6	0.65	0.58	3.75
CDCA Content	THF/EtOH (1:4)	60	2	12.6	0.71	0.67	5.90
Reduce Polarity (Champion Cell)	Tol/EtOH (1:1)	60	2	15.8	0.70	0.70	7.70

6. HRMS of SM63

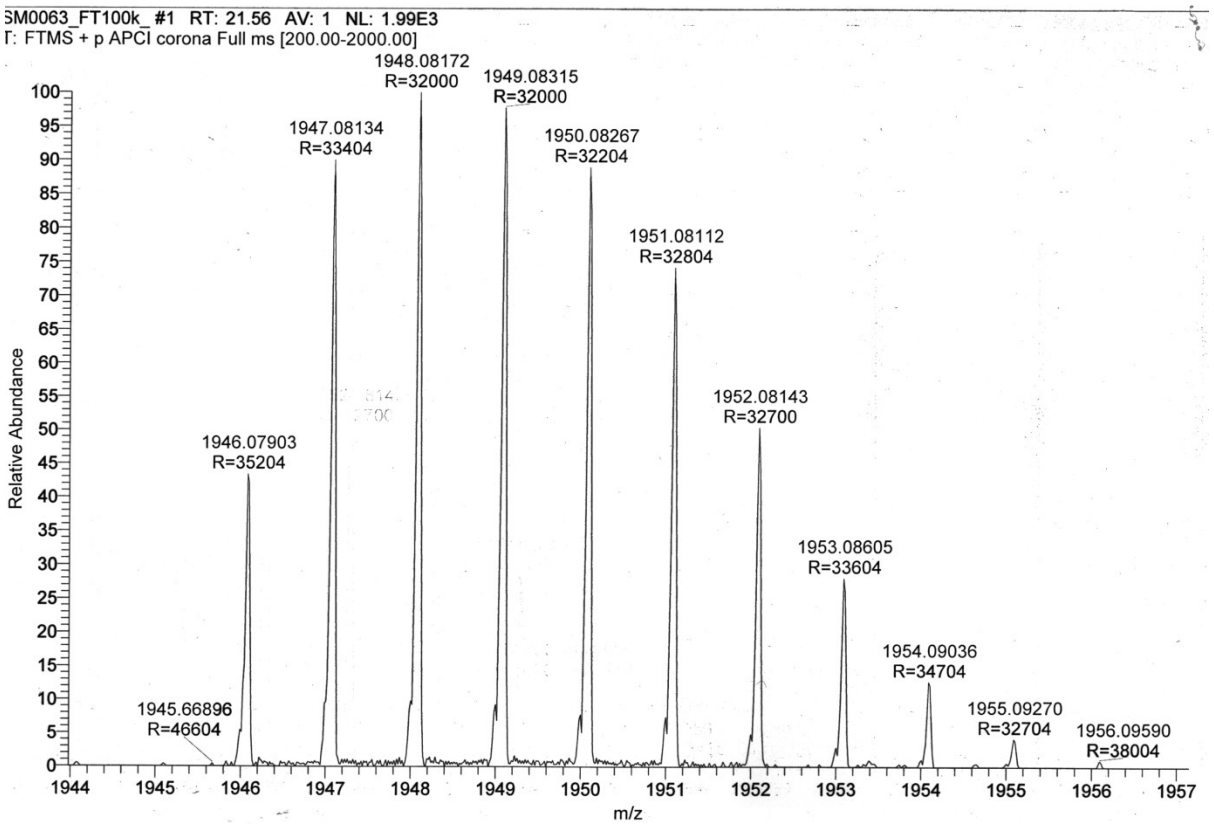

7. ^{1}H NMR of SM63

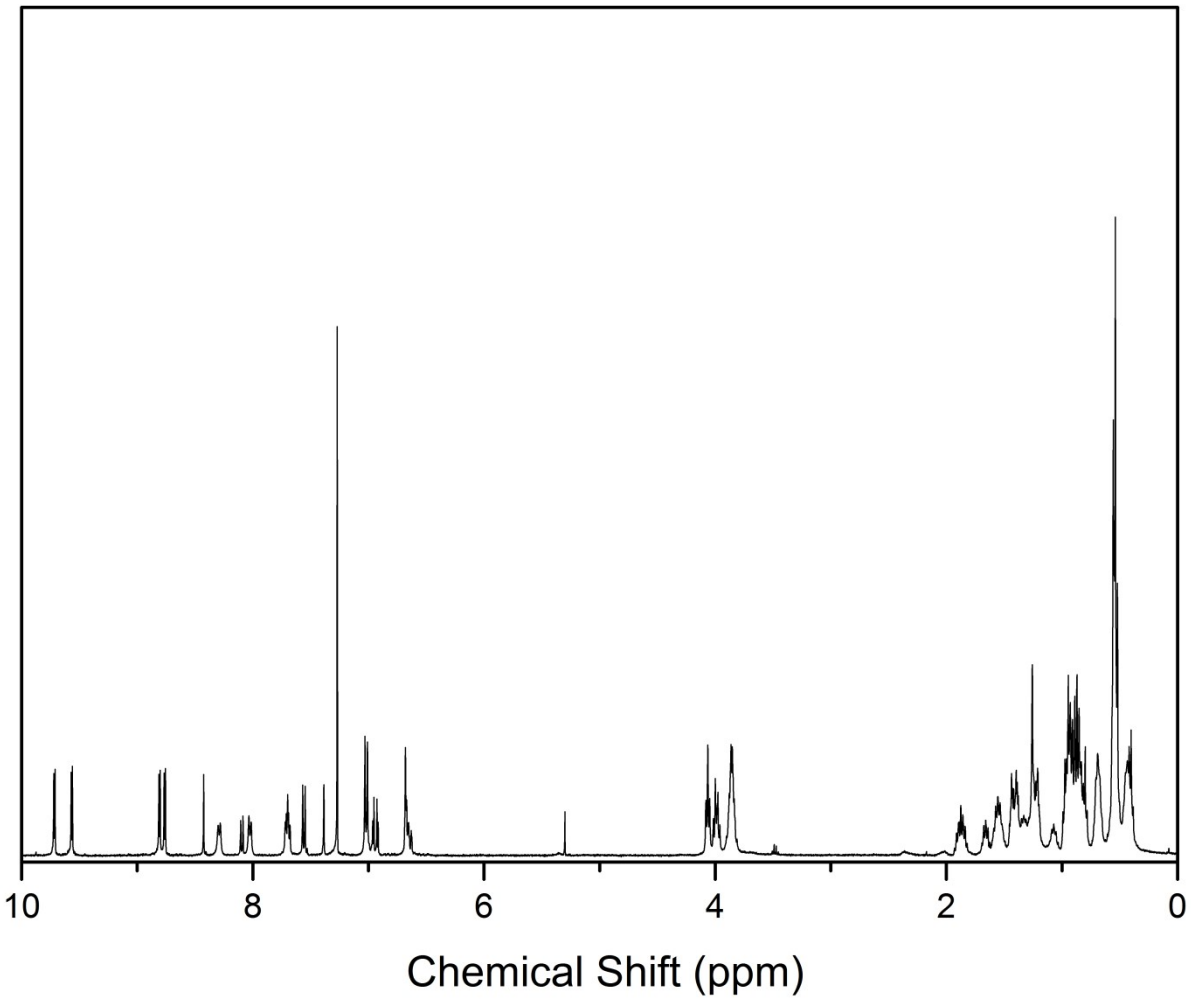

8. ^{13}C NMR of SM63

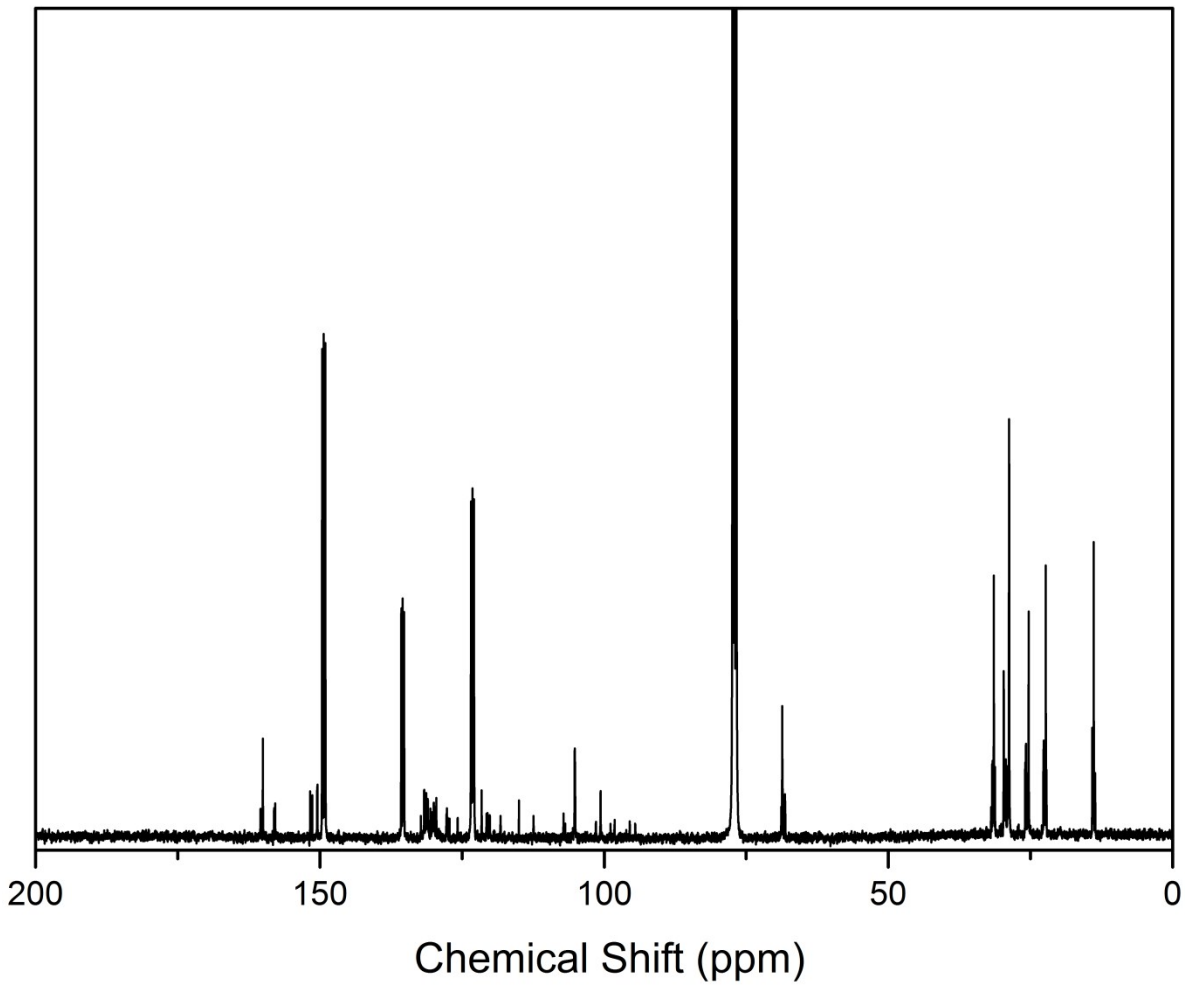

9. References

1. F. Dolhem, C. Lièvre, G. Demailly, *Tetrahedron*, 2003, **59**, 155–164.
2. J. H. Delcamp, A. Yella, T. W. Holcombe, M. K. Nazeeruddin, M. Grätzel M., *Angew. Chem. Int. Ed.*, 2013, **52**, 376–380.
3. C. L. Wang, C. M. Lan, S. H. Hong, Y. F. Wang, T. Y. Pan, C. W. Chang, H. H. Kuo, M. Y. Kuo, E. W. G. Diau, C. Y. Lin, *Energy. Environ. Sci*., 2012, **5**, 6933–6940.
4. Y. Zhao and D. G. Truhlar, *Theor. Chem. Acc*., 2008, **120**, 215–241.
5. T. H. Dunning Jr. and P. J. Hay, in Modern Theoretical Chemistry, Ed. H. F. Schaefer III, Vol. 3 (Plenum, New York, 1977) 1–28.
6. R. Ditchfield, W. J. Hehre, and J. A. Pople, *J. Chem. Phys*., 1971, **54**, 724–728.
7. M. J. Frisch, G. W. Trucks, H. B. Schlegel, G. E. Scuseria, M. A. Robb, J. R. Cheeseman, G. Scalmani, V. Barone, B. Mennucci, G. A. Petersson, H. Nakatsuji, M. Caricato, X. Li, H. P. Hratchian, A. F. Izmaylov, J. Bloino, G. Zheng, J. L. Sonnenberg, M. Hada, M. Ehara, K. Toyota, R. Fukuda, J. Hasegawa, M. Ishida, T. Nakajima, Y. Honda, O. Kitao, H. Nakai, T. Vreven, J. A. Montgomery, Jr., J. E. Peralta, F. Ogliaro, M. Bearpark, J. J. Heyd, E. Brothers, K. N. Kudin, V. N. Staroverov, R. Kobayashi, J. Normand, K. Raghavachari, A. Rendell, J. C. Burant, S. S. Iyengar, J. Tomasi, M. Cossi, N. Rega, J. M. Millam, M. Klene, J. E. Knox, J. B. Cross, V. Bakken, C. Adamo, J. Jaramillo, R. Gomperts, R. E. Stratmann, O. Yazyev, A. J. Austin, R. Cammi, C. Pomelli, J. W. Ochterski, R. L. Martin, K. Morokuma, V. G. Zakrzewski, G. A. Voth, P. Salvador, J. J. Dannenberg, S. Dapprich, A. D. Daniels, Ö. Farkas, J. B. Foresman, J. V. Ortiz, J. Cioslowski and D. J. Fox, Gaussian Inc., Wallingford CT, 2009. Gaussian 09, Revision A.02. Gaussian, Inc.: Wallingford CT, 2009.
8. J. Tomasi, B. Mennucci, R. Cammi, *Chem. Rev*., 2005, **105**, 2999–3094.
9. S. Mathew, A. Yella, P. Gao, R. Humphry-Baker, B. F. E. Curchod, N. Ashari-Astani, I. Tavernelli, U. Rothlisberger, M. K. Nazeeruddin, M. Grätzel, *Nat. Chem*., 2014, **6**, 242–247.
10. W. Humphrey, A. Dalke, K. Schulten, *J. Mol. Graph*. 1996, **14**, 33–38.
11. A. D. Becke, Phys. Rev. A, 1988, **38**, 3098–3100.
12. Y. Zhao and D. G. Truhlar, *J. Chem. Theor. Comput*., 2005, **1**, 415–432.
13. Y. Zhao, D. G. Truhlar, *J. Chem. Theor. Comput*., 2007, **3**, 289–300.
14. S. Grimme, *J. Comp. Chem*., 2006, **27**, 1787–1799.